Parameter Constraints for Virtual Synchronous Generator Considering Stability

Junru Chen, *Student Member, IEEE,* Terence O'Donnell, *Member, IEEE*

***Abstract*— Virtual synchronous generator (VSG) control for converters has been proposed as a method to provide virtual inertia from power electronics connected generation and storage. Most works to date have analyzed VSG control under the assumption that the VSG dynamics are much slower than that the converter. This work shows that when converter and line dynamics are taken into account the virtual inertia and damping settings are constrained by stability considerations. These conditions for stability are analyzed based on a simple transfer function approach. It is shown that for the VSG to be stable and validly approximated by a second order system, the ratio of damping to virtual inertia is a key parameter. This paper quantifies how these VSG parameters are constrained by stability. The transfer function analysis is validated using full switching model simulations of stable and unstable cases.**

***Index Terms*—Virtual Synchronous Generator, Virtual Inertia, Damping, Transfer function, Stability**

I. Introduction

In the context of power systems with higher penetrations of power electronics connected generation, virtual synchronous generator (VSG) control of converters has been proposed as a means to improve the system transient stability by emulating inertia in the control loop of the converter. To obtain clearer insight into the VSG settings most previous works have analyzed the VSG neglecting the effects of the line resonance [1][2] and the voltage source converter (VSC) dynamics [3]. This is valid based on the assumption that the overall VSG response is much slower than either the VSC dynamics or the system synchronous frequency. Under these assumptions the VSG dynamics can be approximated by a second order transfer function thus simplifying the analysis and giving useful insight. Of course, in most cases, this assumption is valid. However, reducing system inertia may demand larger virtual inertial response from converters, thus requiring more rapid power response from the VSG. It is therefore important to understand the range of settings for which the simplified second order analysis remains valid so as to avoid stability problems with the overall VSG response. The original contribution of this work is to provide a simple analysis based on transfer functions which gives insight into the choice of VSG virtual inertia and damping settings to ensure VSG stability taking into consideration VSG, VSC and line dynamics. This has important consequences for the range of virtual inertia and damping response which can be obtained from converter connected generation and storage. The proposed constraints define the necessary and sufficient condition to ensure stability and the validity of the reduced VSG model used in power system level analysis.

This work is funded by the Science Foundation Ireland (SFI) Strategic Partnership Programme Grant Number SFI/15/SPP/E3125.

Junru Chen and T. O'Donnell are with the Electrical Engineering Department, University College Dublin, Dublin 4, Ireland (e-mail: junru.chen.1@ucdconnect.ie, tenrence.odonnell@ucd.ie).

II. Virtual Synchronous Generator

There have been several different previous implementations of the VSG [4][5]. In this letter, we use a relatively common topology, which operates the VSC in the voltage source mode [4] with inner current control and outer voltage control. Besides these relatively standard VSC controls, the VSG control is implemented in outer loops which provide the virtual inertia and damping and can also implement a virtual impedance. The virtual impedance emulates an impedance connected in series with the grid line impedance between the VSC output voltage u_o and the PCC u_g which can be used for R/X ratio modification. The VSG essential parts are shown in the Fig. 1.

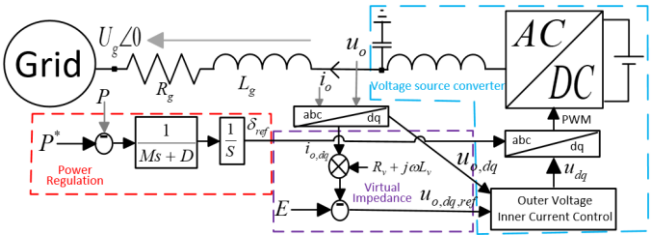

Fig. 1. System structure

Note that some implementations of VSG control consider separate droop and damping terms while others, in order to eliminate the need for a PLL, have combined droop and damping. The analysis here applies to either with the understanding that the constraints apply to the inertia and damping settings.

A. VSG Power regulation

The core function of VSG control is an emulation of the swing equation to determine the phase of the electric potential δ_{ref} by feeding back the real power P as shown in Fig. 1. Taking the grid voltage as reference, the transfer function from power to electric potential angle based on the swing equation is given in (1).

$$G_{PR}(s) = \frac{\delta_{ref}}{\Delta P} = \frac{1}{Ms + D} \cdot \frac{1}{s} \tag{1}$$

where M is the virtual inertia, D is the damping, ΔP is the difference between the output power and its reference. Note, $\frac{M}{D}$ is the time constant for the swing equation. The electric

potential magnitude, *E*, in Fig. 1 is determined by a reactive power control, and is assumed fixed in letter.

B. Voltage Source Converter control

The electric potential, *E*, which is output from the VSG is further processed through a virtual impedance control in order to determine the output voltage u_o. We make the assumption that the virtual impedance has the same effect as an impedance in series with the line impedance. Thus, the obtained electric potential can be presented directly as the reference for the voltage source converter control, which according to [3], has a closed-loop transfer function given by (2).

$$G_{VSC}(s) = \frac{\delta}{\delta_{ref}} = \frac{K_p s + K_i}{C_f t_i s^3 + C_f s^2 + K_p s + K_i} \quad (2)$$

where it is assumed that the closed loop response for the inner current controller can be approximated by a first order response with time constant t_i (normally set to 0.5~5 ms [3]), the outer voltage controller is a PI controller with parameters K_p / K_i, and C_f is the converter filter capacity. According to the procedure in [3], here K_p and K_i are chosen to make the G_{VSC} corner frequency greater than 100 Hz.

C. Line resonance

It has previously been shown that the angle to power transfer across a line impedance has a resonance at the synchronous frequency. Although reference [1] has analysed this resonance for the VSG, it did not include virtual impedance in the analysis. The virtual impedance $R_v + jX_v$connects to the line impedance $R_g + jX_g$ in series to give a combined impedance $R + jX$. Denoting initial equilibrium point values with subscript "0" i.e. E_0, U_{g0}, δ_0 and using similar analysis as detailed in [1] and [2], we can obtain the transfer function for the output power at u_o point in Fig. 1 to the electric potential phase angle δ.

$$H_{Line}(s) = \frac{\Delta P}{\Delta \delta} = \frac{3E_0}{2} \frac{a_1 s^2 + a_2 s + a_3}{(R^2 + X^2)[(R + sL)^2 + X^2]} \quad (3)$$

where $a_1 = U_{g0} L L_g (R sin\delta_0 + X cos\delta_0) - E_0 L X L_g$;
$a_2 = 2U_{g0} L r_g (R sin\delta_0 + X cos\delta_0) - 2E_0 L X r_g - U_{g0} L_v sin\delta_0 (R^2 - X^2) + 2E_0 L_v X sin\delta_0 (R sin\delta_0 - X cos\delta_0)$;
$a_3 = U_{g0}(R^2 + X^2)(R sin\delta_0 + X cos\delta_0) - 2U_{g0} R_v R^2 sin\delta_0 + 2E_0 R_v X sin\delta_0 (R sin\delta_0 - X cos\delta_0)$.

The poles of (3) are at $-\frac{R}{L} \pm j\omega_g$, from which is can be seen that line resonance occurs at ω_g, the grid synchronous frequency, at which the phase changes from 0° to -180°. On the other hand, in the low frequency range, i.e. *s*=0, (3) acts as a gain (4) to the VSG system.

$$H_{Line,0} = \frac{3}{2} \frac{E_0 a_3}{(R^2 + X^2)^2} \quad (4)$$

D. Overall VSG Transfer Function

The entire VSG transfer function from change in power reference (coming from either DC source generation and/or frequency to power droop) to change in output real power is the combination of of G_{PR}, G_{VSC} and $H_{Line}(s)$ as shown in (5).

$$G_{VSG}(s) = G_{PR}(s) \cdot G_{VSC}(s) \cdot H_{Line}(s) \quad (5)$$

The crossover frequency for the VSC is higher than the grid synchronous frequency ω_g. Therefore, in low frequency, the VSC part can be neglected as it has unity gain and zero phase shift, while the line resonance has a gain $H_{Line,0}$. The dominant part is the VSG power regulation with a pole at zero and a pole at $-\frac{D}{M}$.Therefore, the VSG transfer function in the low frequency range can be approximated to a second order system given by (6) with cross-over frequency (7).

$$G_{VSG2}(s) = G_{PR} \cdot H_{Line,0} = \frac{H_{Line,0}}{Ms^2 + Ds} \quad (6)$$

$$\omega_{co} = \sqrt{\frac{-D^2 + \sqrt{D^4 + 4M^2 H_{Line,0}^2}}{2M^2}} \quad (7)$$

Most previous work on VSG only considered (6), which yields useful insights into the required settings for virtual inertia and damping. However, to ensure that (6) is a good approximation and to ensure the stability of the VSG system, the crossover frequency (7) should ideally be placed 10 times below the grid synchronous frequency ω_g in order to remove the effects of line resonance, which could result in pushing the phase below -180°. In addition another consideration for stability is that the crossover frequency of $G_{VSG2}(s)$ (6) should be placed below $\frac{D}{M}$ in order to ensure the slope at crossover is -20 dB/decade. Note, when $0.1\omega_{co} \leq \frac{D}{M} \leq \omega_{co}$ the system is poorly stable. The condition for ensuring stability with adequate phase margin can be summarized as:

$$\begin{cases} \omega_{co} \leq 0.1\omega_g \\ \omega_{co} \leq \frac{D}{M} \end{cases} \quad (8)$$

In order to fulfill conditions (8), considering (7), the way to enhance system stability is to reduce the gain $H_{Line,0}$and/or increase the damping gain *D* assuming a fixed virtual inertia. Reduction of the gain $H_{Line,0}$can be achieved by an increase in virtual impedance assuming the line impedance cannot be easily changed. From these considerations, the ratio, $\frac{D}{M} \geq 0.1\omega_g$ would be a secure selection for *M* and *D* to ensure VSG stability.

III. VALIDATION EXAMPLE

As an example a 10 kV, 1 MW VSG connected to a 50 Hz grid is used to illustrate the proposed VSG stability constraints in Matlab/Simulink. The tests include 3 cases as follows:

- Case 1, stable with $\omega_{co} = 17.4$ rad/s, $\frac{D}{M} = 61.2$rad/s So that $\omega_{co} < \frac{D}{M}$, while $\omega_{co} < 0.1\omega_g$ satisfying both conditions in (8)
- Case 2: unstable with, $\omega_{co} = 414.2$ rad/s and $\frac{D}{M} = 612.1$ rad/s, $\frac{D}{M} > \omega_{co}$, while $\omega_{co} > 0.1\omega_g$
- Case 3: unstable with, $\omega_{co} = 33.0$ rad/s and $\frac{D}{M} = 6.1$ rad/s, so that $\frac{D}{M} < \omega_{co}$, while $\omega_{co} < 0.1\omega_g$

The initial equilibrium points are $E_0 = U_{g0} = 8.165\,kV$, $\delta_0 = 0$. The line impedance and virtual inertia is identical in all cases, i.e. $R_g = 0.0124\,\Omega$, $L_g = 0.1\,H$, $M = 2600$. The VSC voltage control P/I gains are 0.02/4.36, current control

P/I gains are 95.5/326.6 and LC filter impedance is 47 mH/29 μF. Fig. 2 to Fig. 4 are the bode plot of the cases including the plot for the line transfer (blue), VSG power regulation (green), VSC (cyan), full VSG (red) and second order VSG (black), where the points indicate the stability margins.

Fig.2 shows the bode plot of the stable case 1, where the crossover frequency is 17.4 rad/s with 74.1° phase margin (point A), while the blue line in Fig. 5 is the time domain result obtained from the Matlab/Simulink EMT simulation of the system with full switching model of the converter. As indicated by the red line, the VSG system is stable. In this case, the VSC transient as expected can be neglected (see cyan line) and the line resonance can be simplified as a gain $H_{Line,0}$. Thus, in low frequency, the approximated second order VSG bode plot (see black line) overlaps the precise VSG system in the range of interest.

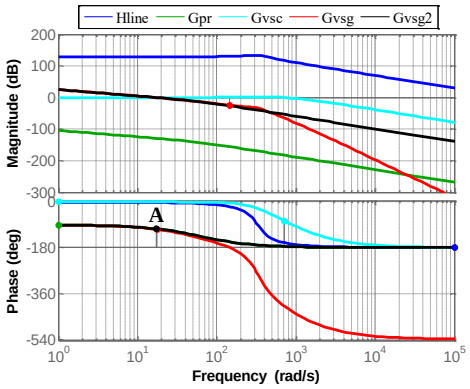

Fig. 2. Bode plot: stable case 1 with VSG crossover frequency 17.4 rad/s, $L_v = 0$ H, $R_v = 10\ \Omega$, $D = 159150$, $\frac{D}{M} = 61.2$rad/s

Fig.3 is the bode plot of the unstable case 2, where the crossover frequency is 414.2 rad/s, while the black line in Fig. 5 is the time domain result. In this case the precise VSG bode plot shows the system to be unstable (point A), while the reduced VSG bode plot indicates stability (point B) with 56° phase margin. The gain margin (point C) of precise VSG is -18.1dB at 286 rad/s or 45.5 Hz, which gives rise to VSG oscillation at this frequency as shown in Fig. 5. This validates the fact that placing the crossover frequency too close to the grid frequency results in a significant contribution from line resonance which leads to the VSG system being unstable.

Fig.4 presents the bode plots for the unstable case 3, while the red line in Fig. 5 is the time domain result. In this case, $\frac{D}{M} < \omega_{co}$, while $\omega_{co} < 0.1\omega_g$. From the result, both precise and reduced VSG transfer function bode plots show that the system is unstable (point A) with 6.8° phase margin and -40 dB/decade crossover slope. The crossover frequency is 33 rad/s or 5.25 Hz, which gives rise to VSG oscillation at this frequency as shown in Fig. 5.

IV. Conclusion

This letter proposes and validates constraints for stable VSG settings considering the VSC dynamics and line resonance effect. It is concluded that the crossover frequency of the reduced VSG transfer function should be placed 10 times below the synchronous frequency, and the damping gain to virtual inertia ratio should be greater than the crossover frequency. These constraints are necessary and sufficient to ensure validity of results obtained using VSG large signal analysis which neglects the VSC transient and line resonance.

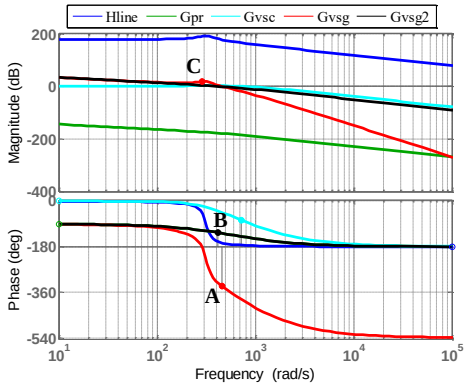

Fig. 3. Bode plot: unstable case 2 with VSG crossover frequency 414.2 rad/s, $L_v = -0.1$ H, $R_v = 0\ \Omega$, $D = 1591500$, $\frac{D}{M} = 612.1$ rad/s.

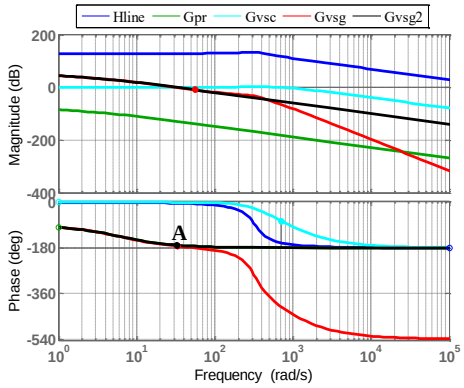

Fig. 4. Bode plot: unstable case 3 with VSG crossover frequency 33.0 rad/s, $L_v = 0$ H, $R_v = 10\ \Omega$, $D = 15915$, $\frac{D}{M} = 6.1$ rad/s.

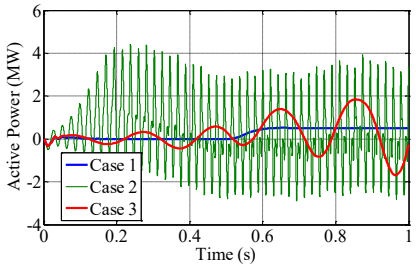

Fig. 5. Time domain results, reference active power step change to 0.5 MW.

V. References

[1] J. Wang *et al.*, "Synchronous Frequency Resonance of Virtual Synchronous Generators and Damping Control", 2015 9th International Conference on Power Electronics and ECCE Asia, pp. 1011 - 1016,2015.

[2] L. Zhang, L. Harnefors and H. Nee, "Power-Synchronization Control of Grid-Connected Voltage-Source Converters," in *IEEE Transactions on Power Systems*, vol. 25, no. 2, pp. 809-820, May 2010.

[3] A. Yazdani and R. Iravani, "Voltage-sourced Converters in Power System," WILEY IEEE PRESS, Mar. 2010, ISBN: 978-0-470-52156-4.

[4] S. Arco, J. A. Suul and O. B. Fosso, "A Virtual Synchronous Machine implementation for distributed control of power converters in Smart Grids," *Electric Power Systems Research*, Vol. 122, pp. 180-197, May 2015.

[5] Y. Cao *et al.*, "A Virtual Synchronous Generator Control Strategy for VSC-MTDC Systems," in *IEEE Transactions on Energy Conversion*, vol. 33, no. 2, pp. 750-761, June 2018.